

Gradient-informed basis adaptation for Legendre Chaos expansions

Panagiotis A. Tsilifis

CSQI, Institute of Mathematics

School of Basic Sciences

École Polytechnique Fédérale de Lausanne

CH-1015 Lausanne, Switzerland

Email: panagiotis.tsilifis@epfl.ch

ABSTRACT

The recently introduced basis adaptation method for Homogeneous (Wiener) Chaos expansions is explored in a new context where the rotation/projection matrices are computed by discovering the active subspace where the random input exhibits most of its variability. In the case where a 1-dimensional active subspace exists, the methodology can be applicable to generalized Polynomial Chaos expansions, thus enabling the projection of a high dimensional input to a single input variable and the efficient estimation of a univariate chaos expansion. Attractive features of this approach, such as the significant computational savings and the high accuracy in computing statistics of interest are investigated.

1 Introduction

While new technological advancements and the rapid increase of computational power simply seem to motivate the need for solving even more complex physical problems, uncertainty quantification (UQ) tasks seem to suffer from the never-ending challenge of the “relatively” limited computational resources available to the experimenter. To overcome this challenge of developing problem- and computer code-independent efficient methodologies that will enable experimentation and predictive capabilities, one necessarily focuses on further advancing the mathematical and algorithmic tools for quantifying the various forms of uncertainties and their effects on physical models.

Most standard UQ approaches involve the use of Monte Carlo (MC) methods [1] where several samples are drawn according to the model input distribution and their corresponding outputs are used to compute certain statistics of interest. The use of such methods typically varies from uncertainty propagation problems [2] to calibration problems [3, 4] to stochastic optimization [5, 6] and experimental design problems [7, 8]. The slow convergence of the method along with the usually expensive computational models can easily make the approach unaffordable and infeasible, causing one to resort to cheaper alternatives. These consist of substituting the computational model with a surrogate that can be repeatedly evaluated at almost no cost, therefore accelerating computations. Such surrogates can be, for instance, polynomial chaos expansions (PCE) [9, 10, 11, 12], Gaussian Processes [13, 14] or adaptive sparse grid collocation [15]. The common characteristic in all the above constructions is that an initial set of forward evaluations at preselected points is used to construct a functional approximation of the original computational model. After such an approximation becomes available, one no longer relies on the expensive-to-evaluate computer code but instead uses the surrogate. Although this characteristic generally outperforms MC methods, it can still fail to address the issue of computational efficiency due to the *curse of dimensionality* effect, that is the increase of the dimensionality of the uncertain input results in an exponentially increasing number of evaluations required to compute the surrogate parameters.

Several ways to achieve dimensionality reduction have been proposed in the literature, among which are sensitivity analysis methods [16] that rank the inputs according to their influence, thus allowing to neglect the components with respect to which, the output is insensitive. These methods involve for example variance decomposition methods such as the Sobol’ indices [17, 18]. Similar approaches might consist of spectral methods, such as the Karhunen-Loève expansion (KLE) [19, 20, 9] for random vectors and random fields, where one expands in a series of scalar variables, the importance of which is determined by the eigenvalues of the covariance matrix. The series can be truncated accordingly, leaving out the unimportant scales of fluctuation of the random quantity. For an empirical version of the KLE one might also consider

the Principal Component Analysis (PCA) [21] or the kernel PCA [22]. At last, one can proceed with the active subspace (AS) method [23, 24, 25] of discovering the low-dimensional projection of the random input space where the model exhibits maximal variability. This makes use of a spectral decomposition of the covariance of the gradient vector, the eigenvectors of which reveal the projection mapping to the active subspace.

In this work, our attention is focused on reduction methods that are applicable on Polynomial Chaos expansions. PCE's provide an analytic and compact representation of the model output in terms of a number of scalar random variables, typically referred to as the germs, through polynomials that are pairwise orthogonal with respect to inner product (expectation) of the underlying Hilbert space of square integrable random variables. Their use, pioneered by [9], has been explored throughout several contexts and applications such as flow through heterogeneous porous media [26, 27], fluid dynamics [28, 29, 30] aeroelasticity [31] etc. for either forward propagation [32, 33] or inference problems [34, 35, 36].

Most of the aforementioned dimensionality reduction methods can be applied on PCE's once the expansion becomes known. In [37, 38], explicit formulas for the Sobol' sensitivity indices were derived with respect to the coefficients of chaos expansions, thus enabling the fast computation of variance decomposition factors whenever such expansions are available. The idea was used in the context of stochastic differential equations [39] to separate the influence of uncertainty due to random paramters from that caused by the driving white noise and in a similar fashion it has also been applied to large-eddy simulations [40] for sensitivity analysis due to turbulent effects. However, the key challenge of reducing the dimensionality of the input, in order to make the computation of the coefficients a feasible task still remains unsolved and most of the works still focus their attention on simply obtaining sparse representations by adaptive finite elements [41], ℓ_1 -minimization [42, 43] and compressive sensing [44].

Recently [45] it was observed that for Hermite expansions with Gaussian input variables, the original input can be rotated using isometries onto the underlying Gaussian Hilbert space to obtain expansions with respect to the new basis that concentrate their dependence on only a few components. Certain choices for the rotation matrix were analytically seen not only to guarantee certain levels of sparsity in the expansion but even concentrate the probabilistic behavior of scalar quantities of interest (QoI) on low-dimensional Gaussian subspaces. Computational schemes for efficiently computing the coefficients of the adapted expansion were also developed and the numerical results were impressive. The basis adaptation concept was further extended from scalar QoI's to random fields [46], where explicit formulas for computing the coefficients with respect to any rotation were derived and the case of a parametric family of rotations was discussed that gives rise to expansions with a Gaussian process input. Even though the idea of rotating the basis has been further applied to design optimization problems [47] and has been used to develop efficient schemes coupled with compressing sensing methods [48, 49], it is still quite restricted to the Homogeneous Chaos expansions, where the Gaussian distribution remains invariant under rotations, a property that is not valid in other cases.

The key difference when applying the above idea in random vectors other than Gaussians, is that the distribution or the rotated variables is, in general, not analytically available and the construction of polynomials, orthogonal with respect to this distribution is not an easy task. In this paper we are exploring the special case where an isometry can be used to rotate the basis in the same fashion as in the basis adaptation methodology, such that only a 1-dimensional component of the new variables will suffice to build an accurate polynomial chaos expansion. In this, quite restrictive case, the input can easily be mapped to a uniform distribution via its own cumulative distribution function and therefore the Legendre polynomials can be used to expand the series. To find the proper rotation matrix, we make use of the active subspace methodology that successfully discovers the rotation such that maximal variability can be achieved in one only variable. To do so, unlike the traditional active subspace method where the covariance matrix of the gradient vector is computed via MC methods, we make use of an initial chaos expansion that is obtained using low-order quadratures, that is with very few model evaluations. In this case the matrix can be analytically computed at no additional cost. Once the active subspace is revealed, a new one-dimensional Legendre chaos expansion of relatively high order can be easily constructed as again, it does not demand many evaluations. Apart from the fact that the approach enables surrogate construction of expensive models that would be otherwise infeasible, we also discover some attractive features: The capability of obtaining high order one-dimensional expansions allows for very accurate predictions of the probabilistic behavior of QoI's where a lower order full-dimensional expansion fails.

This paper is structured as follows: Section 2 reviews the polynomial chaos and active subspace approaches and then presents how the first can be used to analytically compute the latter along with an algorithm for efficient construction of 1d Legendre Chaos expansions. In Section 3 we apply the methodology to two numerical examples. First, a simple quadratic polynomial function with analytically known active subspace is used for validation and second, a multiphase flow problem that simulates transport of ammonium and its oxidation to nitrite along a 1-dimensional rod is used to draw my conclusions.

2 Methodology

To provide a proper setting upon which our methodology is developed, we first consider a general response function $f : D \subset \mathbb{R}^d \rightarrow \mathbb{R}$ where the points $\xi \in D$ will be thought of as *inputs* and their mappings $f(\xi)$ will be the *model outputs* or the *quantity of interest (QoI)*. Typically D is also equipped with some probability measure \mathbb{P} therefore its elements are D -valued

random variables from a space of events Ω to D . A σ -algebra \mathcal{F} that consists of the \mathbb{P} -measurable subsets of Ω or in other words, the inverse mappings of the Borel subsets of D is naturally defined and thus the probability triplet $(\Omega, \mathcal{F}, \mathbb{P})$ is the space on which we will be working.

2.1 Generalized Polynomial Chaos

Throughout this paper we will assume that the quantity $f(\xi)$ has finite variance and therefore is a square integrable function, that is $f \in L^2(\Omega, \mathcal{F}, \mathbb{P})$. It is known then [10], that f admits a series expansion in terms of orthogonal polynomials of ξ , given as

$$f(\xi) = \sum_{\alpha, |\alpha|=0}^{\infty} f_{\alpha} \psi_{\alpha}(\xi), \quad (1)$$

where $\alpha = (\alpha_1, \dots, \alpha_d) \in \mathcal{J} := \mathbb{N} \cup \{\mathbf{0}\}$ are finite-dimensional multiindices with norm $|\alpha| = \alpha_1 + \dots + \alpha_d$ and ψ_{α} are d -dimensional polynomial functions of ξ that are orthogonal with respect to the measure defined by the density function $p(\xi)$, that is

$$\mathbb{E}\{\psi_{\alpha}(\xi)\psi_{\beta}(\xi)\} = \int_D \psi_{\alpha}(\xi)\psi_{\beta}(\xi)p(\xi)d\xi = \|\psi_{\alpha}\|^2 \delta_{\alpha,\beta} \quad (2)$$

where $\|\psi_{\alpha}\| = (\mathbb{E}\{\psi_{\alpha}(\xi)^2\})^{1/2}$ and $\delta_{\alpha,\beta}$ is the Dirac delta function which is 1 if $\alpha = \beta$ and 0 otherwise. Without loss of generality we assume here that $\|\psi_{\alpha}\| = 1$, that is the polynomials are normalized. We will refer to eq. (1) as the *polynomial chaos (PC) expansion* of f . In the case where $\xi = (\xi_1, \dots, \xi_d)$ consists of independent and identically distributed random variables, the polynomials are expanded as

$$\psi_{\alpha} = \prod_{i=1}^d \psi_{\alpha_i}(\xi_i) \quad (3)$$

where $\psi_{\alpha_i}(\xi_i)$ are univariate polynomials of ξ_i of order α_i , $i = 1, \dots, d$. Common choices of the density function $p(\xi) = \prod_{i=1}^d p(\xi_i)$ give rise to known forms of the polynomials, for instance the Gaussian, Uniform, Gamma and Beta distributions correspond to Hermite, Legendre, Laguerre and Jacobi polynomials respectively [10].

In practice, we work with truncated versions of (1), that is for $Q \in \mathbb{N}$, $\mathcal{J}_Q := \{\alpha \in \mathcal{J} : |\alpha| \leq Q\}$, we will assume that f can be *accurately* approximated by

$$f(\xi) \approx \sum_{\alpha \in \mathcal{J}_Q} f_{\alpha} \psi_{\alpha}(\xi). \quad (4)$$

The above expansion consists of

$$N_Q = \binom{d+Q}{Q} = \frac{(d+Q)!}{d!Q!} \quad (5)$$

basis terms and the estimation of the corresponding coefficients is typically a challenging task. Several approaches have been developed in the literature for the estimation of the coefficients $\{f_{\alpha}\}_{\alpha \in \mathcal{J}_Q}$, divided in two main categories: Intrusive and non-intrusive methods. The first, pioneered by [9], treats the solution of a differential equation as a random field that can be written as in (4), where the coefficients vary as functions of the spatial or time parameters associated with the computational domain. The expression is then substituted in the equation satisfied by f , in order to derive the governing equations satisfied by the coefficients, which then need to be solved once. Non-intrusive approaches involve estimation of the coefficients using the relation

$$f_{\alpha} = \mathbb{E}\{f(\xi)\psi_{\alpha}(\xi)\} \quad (6)$$

which is computed using numerical integration techniques. As mentioned in the previous section, both approaches suffer by the curse of dimensionality which in the first case implies that the system of equations to be solved increases exponentially as a function of the dimensionality d and in the second case, the exponential increase is on the number of collocation points where the model f needs to be evaluated.

2.2 Active subspaces

2.2.1 Discovering the active subspace

Let us assume that the function f can be well-approximated by

$$f(\xi) \approx g(\mathbf{W}^T \xi) \quad (7)$$

where \mathbf{W} is a $d \times d'$ matrix with orthonormal columns, that is it satisfies

$$\mathbf{W}^T \mathbf{W} = \mathbf{I}_{d'} \quad (8)$$

and $g : \mathbb{R}^{d'} \rightarrow \mathbb{R}$ is a d' -dimensional function that will be called the *link* function. Intuitively, such an assumption implies that the domain D can be rotated using a $d \times d$ orthonormal matrix

$$\mathbf{A} = [\mathbf{W} \mathbf{V}] \quad (9)$$

with $\mathbf{A}^T \mathbf{A} = \mathbf{I}_d$ and \mathbf{W}, \mathbf{V} being $d \times d'$ and $d \times (d - d')$ matrices respectively such that f exhibits most of its variation on the space spanned by $\{\mathbf{W}^T \xi : \xi \in D\}$ while it remains insensitive to variations on its orthogonal complement, thus motivating the term *active subspace* [23].

As it is clear from the above, the main challenge in the above construction is the determination of the *rotation* matrix \mathbf{A} such that the active subspace defined by \mathbf{W} will have the minimum possible dimensionality d' . To explore the directions along which f exhibits greatest sensitivity, we define the $d \times d$ matrix

$$\mathbf{C} = \mathbb{E} \{ \nabla f(\xi) \nabla f(\xi)^T \}, \quad (10)$$

where $\nabla f(\xi) = \left(\frac{\partial f(\xi)}{\partial \xi_1}, \dots, \frac{\partial f(\xi)}{\partial \xi_d} \right)^T$ is the gradient vector of f . This is essentially the uncentered covariance matrix of $\nabla f(\xi)$ and is a symmetric and positive semi-definite matrix, therefore it admits a decomposition as

$$\mathbf{C} = \mathbf{U} \mathbf{\Lambda} \mathbf{U}^T, \quad (11)$$

where $\mathbf{\Lambda}$ is the diagonal matrix with entries the eigenvalues of \mathbf{C} in decreasing order, namely $\lambda_i, i = 1, \dots, d$ with $\lambda_1 \geq \dots \geq \lambda_d$ and \mathbf{U} is the unitary matrix whose i th column is the eigenvector of \mathbf{C} corresponding to λ_i . By setting $\mathbf{A} = \mathbf{U}$ and $\eta = \mathbf{A}^T \xi$ it can be shown [23] that

$$\mathbb{E} \{ \nabla_{\eta} f)^T (\nabla_{\eta} f) \} = \lambda_1 + \dots + \lambda_d \quad (12)$$

and by decomposing \mathbf{A} as in (9) and setting $\eta_{\mathbf{w}} = \mathbf{W}^T \xi$ gives us that the mean-squared gradients of f with respect to $\eta_{\mathbf{w}}$ will be the sum of the d' largest eigenvalues. This construction provides us a way of rotating the input space D and separating it into two subspaces namely the active subspace and its orthogonal complement by simply selecting the d' most dominant eigenvalues of \mathbf{C} and their corresponding eigenvectors. Then the function f can be approximated as in eq. 7.

2.2.2 Active subspace computation for PC expansions and reduction to univariate Legendre Chaos

The key challenge in the active subspace methodology is the computation of the *gradient matrix* \mathbf{C} , the standard way of which is by estimating the expectation using Monte Carlo sampling. Recently a gradient-free approach for determining the projection matrix when f is approximated by a Gaussian Process was developed [50]. For this purpose, assume that a PC expansion is available for f as in eq. (4). Then \mathbf{C} can be written as

$$\mathbf{C} \approx \mathbb{E} \left\{ \nabla \left(\sum f_{\alpha} \psi_{\alpha}(\xi) \right) \cdot \nabla \left(\sum f_{\beta} \psi_{\beta}(\xi) \right)^T \right\} \quad (13)$$

and the entries C_{ij} will be given by

$$\begin{aligned}
C_{ij} &\approx \mathbb{E} \left\{ \frac{\partial}{\partial \xi_i} (\sum_{\alpha} f_{\alpha} \psi_{\alpha}(\xi)) \cdot \frac{\partial}{\partial \xi_j} (\sum_{\beta} f_{\beta} \psi_{\beta}(\xi))^T \right\} \\
&= \mathbb{E} \left\{ \left(\sum_{\alpha} f_{\alpha} \frac{\partial \psi_{\alpha}(\xi)}{\partial \xi_i} \right) \cdot \left(\sum_{\beta} f_{\beta} \frac{\partial \psi_{\beta}(\xi)}{\partial \xi_j} \right)^T \right\} \\
&= \sum_{\alpha} \sum_{\beta} f_{\alpha} f_{\beta} \mathbb{E} \left\{ \frac{\partial \psi_{\alpha}(\xi)}{\partial \xi_i} \cdot \frac{\partial \psi_{\beta}(\xi)}{\partial \xi_j} \right\} \\
&= \mathbf{f}^T \mathbf{K}_{ij} \mathbf{f}
\end{aligned} \tag{14}$$

where \mathbf{K}_{ij} is the *stiffness* matrix with entries

$$(\mathbf{K}_{ij})_{\alpha\beta} = \mathbb{E} \left\{ \frac{\partial \psi_{\alpha}(\xi)}{\partial \xi_i} \cdot \frac{\partial \psi_{\beta}(\xi)}{\partial \xi_j} \right\} \tag{15}$$

and $\mathbf{f} = \{f_{\alpha}\}_{\alpha \in \mathcal{J}_Q}$ is the vectorized representation of the chaos coefficients. The values of the entries of the stiffness matrices \mathbf{K}_{ij} , $i, j = 1, \dots, d$ depend solely on the polynomials used in the PC expansion and their corresponding probability measures with respect to which the expectation is taken and can be computed independently of the nature of the function f . Detailed computation of \mathbf{K}_{ij} of the case of Legendre polynomials is provided in Appendix A. Computation of \mathbf{C} generally requires full knowledge of the coefficients \mathbf{f} and can be an expensive task. However, as we describe in the next section, a relatively *cheap* estimation of the coefficients, based on low level quadrature rules can suffice of this purpose.

Let us now assume that the matrix \mathbf{C} is available and that $\lambda_1 \gg \lambda_2$. This implies that the rotation matrix \mathbf{A} can be decomposed in a 1-dimensional vector \mathbf{w} with $\mathbf{w}^T \mathbf{w} = 1$ and a $d \times (d-1)$ matrix \mathbf{V} such that f exhibits most of its variation on the space spanned by $\eta = \mathbf{w}^T \xi$ and can be accurately approximated as a function of η as in eq. (7). The square integrability condition of f directly implies that f can be expanded in a polynomial chaos expansion in terms of polynomials that are orthogonal with respect to the probability measure of η . To avoid the structure of such polynomials, since the probability measure $p(\eta)d\eta$ can be arbitrarily complex, we introduce the uniform $\mathcal{U}(-1, 1)$ germ

$$\zeta = 2F_{\eta}(\eta) - 1, \tag{16}$$

where $F_{\eta}(\cdot)$ is the cumulative probability distribution of η and we write

$$f(\xi) \approx g(\eta) = g \left(F_{\eta}^{-1} \left(\frac{\zeta + 1}{2} \right) \right) := g(\zeta). \tag{17}$$

Finally g can be expanded as

$$g(\zeta) = \sum_{n=0}^{N_{\zeta}} g_n \psi_n(\zeta) \tag{18}$$

where $\psi_n(\zeta)$ are the normalized univariate Legendre polynomials and thus we can achieve a 1-dimensional chaos decomposition of f .

2.3 Efficient basis reduction using pseudo-spectral projections

Using eq. (6) the coefficients of the chaos expansion of f can be estimated after approximating the integral with

$$f_{\alpha} = \int_D f(\xi) \psi_{\alpha}(\xi) p(\xi) d\xi \approx \sum_{i=1}^S f(\xi^{(i)}) \psi_{\alpha}(\xi^{(i)}) w_i, \quad \alpha \in \mathcal{J}_Q, \tag{19}$$

using a quadrature rule $\{\xi^{(i)}, w_i\}_{i=1}^{s_d}$, where $\{\xi^{(i)}\}_{i=1}^{s_d}$ are quadrature points and $\{w_i\}_{i=1}^{s_d}$ are the corresponding weights. As mentioned above, such a procedure can be prohibitive for relatively large d or for computationally expensive models f that

exhibit high nonlinearity. It is desirable, in such cases, to develop a computational strategy that reduces the computational resources by limiting the number of model evaluations. Provided that a 1-dimensional active subspace exists, writing f in the form (18) and computing the coefficients $\{g_n\}_{n=0}^{N_\zeta}$ would be an efficient alternative. Since this requires the knowledge of the projection vector \mathbf{w} , one could perform the following steps: First, a low level quadrature rule that consists of an affordable number of points can be performed in order to compute the low order coefficients $\{f_\alpha\}_{\alpha \in \mathcal{J}_{Q_0}}$, $Q_0 < Q$ and an estimate of \mathbf{C} and therefore of \mathbf{w} can be obtained. Then the PC coefficients of g can be computed in a similar manner by

$$g_n \approx \sum_{i=1}^{s_1} g(\zeta^{(i)}) \psi_n(\zeta^{(i)}) w_i \quad (20)$$

where $\{\zeta^{(i)}\}_{i=1}^{s_1}$ are 1-dimensional quadrature points on the $[-1, 1]$ space. In practice, evaluation of $g(\zeta^{(i)})$ will require transforming $\zeta^{(i)}$ to $\eta^{(i)} = F_\eta^{-1}(\frac{\zeta^{(i)}+1}{2})$ and $\eta^{(i)} = \mathbf{A}\xi^{(i)}$ where $\eta^{(i)}$ is a d -dimensional arbitrary completion of $\eta^{(i)}$, where the remaining $d-1$ entries will essentially play no role in the model output as they span the subspace with respect to which f is approximately invariant. This procedure is summarized in the pseudo-algorithm described in Algorithm 1.

Algorithm 1: Non intrusive implementation

- Input** : Quadrature points and weights $\{\xi^{(i)}, w_i\}_{i=1}^{s_d}$ corresponding to d -dimensional, s_d -point quadrature rule and quadrature points and weights $\{\zeta^{(i)}, w_i\}_{i=1}^{s_1}$, corresponding to 1-dimensional, s_1 -point quadrature rule.
Step 1 : Estimate the coefficients $\{f_\alpha\}_{\alpha \in \mathcal{J}_{Q_0}}$ as in eq. (19).
Step 2 : Compute \mathbf{C} using eq. (14) and find \mathbf{A} and \mathbf{w} such that

$$\mathbf{C} = \mathbf{A}\mathbf{A}^T, \quad \mathbf{A} = [\mathbf{w} \quad \mathbf{V}].$$

- Step 3** : Estimate $F_\eta^{-1}(\cdot)$ and compute $\eta^{(i)} = F_\eta^{-1}(\frac{\zeta^{(i)}+1}{2})$ and

$$\hat{\xi}^{(i)} = \mathbf{w}\eta^{(i)}, \quad i = 1, \dots, s_1.$$

- Step 4** : Evaluate QoI at $\{\hat{\xi}^{(i)}\}_{i=1}^{s_1}$ to obtain $\{f(\hat{\xi}^{(i)})\}_{i=1}^{s_1}$ and estimate the coefficients $\{g_n\}_{n=1}^{N_\zeta}$ as

$$g_n \approx \sum_{i=1}^{s_1} f(\hat{\xi}^{(i)}) \psi_n(\zeta^{(i)}) w_i.$$

For the implementation of the above algorithm in the numerical examples that are presented in this paper, the python package `chaos_basipy` [51] has been used that is equipped with polynomial chaos basis function evaluations capabilities, quadrature points generation and computation of the stiffness matrices \mathbf{K}_{ij} derived above.

2.4 Error analysis

The procedure described so far includes computation of the coefficients of a low order polynomial chaos expansion using an efficient numerical integration scheme, typically a low-level sparse quadrature rule. Although the estimation of the coefficients can be satisfactorily accurate, the computation of the gradient vector covariance matrix and subsequently the computation of the active subspace is still subject to the truncation error introduced by using a low order chaos expansion. Below we attempt to quantify this error by deriving some rather standard upper bounds for error of the covariance estimate and its eigenvalues.

Let us denote with $\hat{f}(\xi)$ the truncated version of $f(\xi)$ to be used for computation of \mathbf{C} ,

$$\hat{f}(\xi) = \sum_{\alpha \in \mathcal{J}_{Q_0}} f_\alpha \psi_\alpha(\xi), \quad (21)$$

where $Q_0 < Q$ and write

$$f(\xi) = \hat{f}(\xi) + \varepsilon(\xi). \quad (22)$$

The error of approximating the gradient can then be written as

$$\nabla_\xi \varepsilon(\xi) = \nabla_\xi f(\xi) - \nabla_\xi \hat{f}(\xi). \quad (23)$$

By defining

$$\gamma_{Q_0} := \|\nabla_\xi \varepsilon(\xi)\|, \quad (24)$$

where $\|\cdot\|$ is the Euclidean norm, we can write

$$\|\nabla_\xi \hat{f}(\xi) - \nabla_\xi f(\xi)\| \leq \gamma_{Q_0}, \quad (25)$$

where clearly $\gamma_{Q_0} \rightarrow 0$ as $Q_0 \rightarrow Q$. Define also

$$\hat{\mathbf{C}} = \mathbb{E} \{ \nabla \hat{f}(\xi) \nabla \hat{f}(\xi)^T \}. \quad (26)$$

By referring to the spectral norm (induced by the Euclidean norm) when $\|\cdot\|$ is applied on matrices, the following Theorem can be stated:

Theorem 1. *The norm of the difference between \mathbf{C} and $\hat{\mathbf{C}}$ is bounded by*

$$\|\hat{\mathbf{C}} - \mathbf{C}\| \leq \mathbb{E} [\gamma_{Q_0}^2] + 2\mathbb{E} [L\gamma_{Q_0}],$$

where $L = \|\nabla_\xi f(\xi)\|$. *Proof.* First note that

$$\begin{aligned} \|\nabla_\xi \hat{f} + \nabla_\xi f\| &= \|\nabla_\xi \hat{f} - \nabla_\xi f + 2\nabla_\xi f\| \leq \\ &\leq \|\nabla_\xi \hat{f} - \nabla_\xi f\| + 2\|\nabla_\xi f\| \leq \gamma_{Q_0} + 2L. \end{aligned} \quad (27)$$

Then we have

$$\begin{aligned} \|\nabla_\xi \hat{f} \nabla_\xi \hat{f}^T - \nabla_\xi f \nabla_\xi f^T\| &= \frac{1}{2} \|(\nabla \hat{f} - \nabla f)(\nabla \hat{f} + \nabla f)^T + (\nabla \hat{f} + \nabla f)(\nabla \hat{f} - \nabla f)^T\| \leq \\ &\leq \|(\nabla \hat{f} + \nabla f)(\nabla \hat{f} - \nabla f)^T\| \leq (\gamma_{Q_0} + 2L)\gamma_{Q_0}. \end{aligned} \quad (28)$$

Finally we get

$$\begin{aligned} \|\hat{\mathbf{C}} - \mathbf{C}\| &= \left\| \mathbb{E} [\nabla_\xi \hat{f} \nabla_\xi \hat{f}^T] - \mathbb{E} [\nabla_\xi f \nabla_\xi f^T] \right\| = \\ &= \left\| \mathbb{E} [\nabla_\xi \hat{f} \nabla_\xi \hat{f}^T - \nabla_\xi f \nabla_\xi f^T] \right\| \leq \mathbb{E} [\|\nabla_\xi \hat{f} \nabla_\xi \hat{f}^T - \nabla_\xi f \nabla_\xi f^T\|] \leq \\ &\leq \mathbb{E} [\gamma_{Q_0}^2] + 2\mathbb{E} [L\gamma_{Q_0}] \quad \square \end{aligned} \quad (29)$$

The following corollary also holds:

Corollary. *The difference between the k th true eigenvalue λ_k and the corresponding estimate θ_k is also bounded as*

$$|\lambda_k - \theta_k| \leq \mathbb{E} [\gamma_{Q_0}^2] + 2\mathbb{E} [L\gamma_{Q_0}].$$

Proof. Simply observe that

$$|\lambda_k - \theta_k| \leq \|\hat{\mathbf{C}} - \mathbf{C}\| \leq \mathbb{E} [\gamma_{Q_0}^2] + 2\mathbb{E} [L\gamma_{Q_0}],$$

where the first inequality follows from Corollary 8.1.6 in [52] and the second from Theorem 1. \square

In the above expressions for the error bounds, we can further write

$$\gamma_{Q_0} = \left\{ \sum_{i=1}^d \left(\sum_{|\alpha|=Q_0+1}^Q f_\alpha \frac{\partial \psi_\alpha(\xi)}{\partial \xi_i} \right)^2 \right\}^{1/2} \quad (30)$$

which gives

$$\mathbb{E}[\gamma_{Q_0}^2] = \sum_{i=1}^d \sum_{|\alpha|=Q_0+1}^Q \sum_{|\beta|=Q_0+1}^Q f_\alpha f_\beta \mathbb{E} \left[\frac{\partial \psi_\alpha(\xi)}{\partial \xi_i} \frac{\partial \psi_\beta(\xi)}{\partial \xi_i} \right] \quad (31)$$

$$= \sum_{i=1}^d \sum_{|\alpha|, |\beta|=Q_0+1}^Q f_\alpha f_\beta (\mathbf{K}_{ij})_{\alpha\beta} \quad (32)$$

$$= \sum_{i=1}^d \sum_{\substack{|\alpha|, |\beta|=Q_0+1 \\ \alpha_{-i}=\beta_{-i}}}^Q f_\alpha f_\beta \left(\prod_{\substack{j=1 \\ j \neq i}}^d \mathbb{E}[\psi'_{\alpha_j}(\xi_j) \psi_{\beta_j}(\xi_j)] \right). \quad (33)$$

In the above, α_{-i} , β_{-i} indicate the multi-indices α , β where the entries α_i , β_i respectively, are excluded and the last line follows by using the expressions for $(\mathbf{K}_{ij})_{\alpha\beta}$, derived in Appendix A. For the second term of the error bound, one can simply use the Cauchy-Schwarz inequality to write $\mathbb{E}[L\gamma_{Q_0}] \leq \mathbb{E}[L^2]^{1/2} \mathbb{E}[\gamma_{Q_0}^2]^{1/2}$ and derive a similar expression for $\mathbb{E}[L^2]$, as above. Further numerical investigation of the behavior of the above error bound falls beyond the scope of this work.

3 Numerical examples

3.1 Polynomial function

Consider the function $f : \mathbb{R}^d \rightarrow \mathbb{R}$ with

$$f(\xi) = a + b\mathbf{w}^T \xi + c\xi^T \mathbf{w} \mathbf{w}^T \xi \quad (34)$$

with constants a, b, c and $\mathbf{w} \in \mathbb{R}^d$ such that $\mathbf{w}^T \mathbf{w} = 1$. For the variables we assume that $\xi = (\xi_1, \dots, \xi_d)$ with ξ_i independent $\mathcal{U}(-1, 1)$. This gives

$$\nabla f(\mathbf{x}) = \mathbf{w} (b + 2c\mathbf{w}^T \xi) \quad (35)$$

which gives

$$\begin{aligned} \mathbb{E} [\nabla f(\xi) \nabla f(\xi)^T] &= \mathbf{w} \mathbb{E} [(b + 2c\mathbf{w}^T \xi)(b + 2c\mathbf{w}^T \xi)] \mathbf{w}^T \\ &= \mathbf{w} \left(b^2 + 4c^2 \mathbb{E} [\xi^T \mathbf{w} \mathbf{w}^T \xi] \right) \mathbf{w}^T \\ &= \mathbf{w} \left(b^2 + \frac{4}{3}c^2 \right) \mathbf{w}^T \end{aligned} \quad (36)$$

and it is clear that $b^2 + \frac{4}{3}c^2$ is the only nonzero eigenvalue corresponding to the eigenvector \mathbf{w} , giving a 1-dimensional active subspace. Setting $\eta = \mathbf{w}^T \xi$ we get

$$f(\xi) = g(\mathbf{w}^T \xi) \quad (37)$$

where the link function $g(\eta)$ is

$$g(\eta) = a + b\eta + c\eta^2. \quad (38)$$

Letting F_η be the cumulative distribution function of η , we are interested in constructing a PC expansion with respect to $\zeta = (2F_\eta(\eta) - 1)$. In our numerical implementation we use arbitrary values for a, b, c and \mathbf{w} that were randomly generated (and are easily reproducible by fixing the random seed) and we take $d = 10$. We have

$$\mathbf{w} = (0.1404, -0.3574, 0.4267, -0.0931, -0.2146, 0.2642, 0.2560, -0.1895, 0.0046, -0.6680)^T \quad (39)$$

and

$$a = 1.1500, b = 0.9919, c = 0.9533. \quad (40)$$

Fig. 1 (left) shows the empirical pdf of η for the above choice of \mathbf{w} and Fig. 1 (right) shows the quadrature points of a level-5 Clenshaw-Curtis rule and their transformed values on the η -space through the mapping $F_\eta^{-1}(\frac{\zeta+1}{2})$. Note here that the expression (34) can be rearranged as a series of Legendre polynomials, therefore its PC expansion is essentially known and has exact order 2. The same expansion can be computed numerically using sparse quadrature rule and specifically, a level-2 rule suffices for an accurate estimation, corresponding to 221 evaluations. Estimation of the coefficients of a 1d PC expansion with respect to ζ using the known orthogonal transformation \mathbf{w} can be achieved using a level-5 rule that corresponds to 33 evaluations of f . Note that the PC expansion with respect to ζ is no longer a 2nd order series. The order of polynomials necessary to achieve convergence here depend on the nature of the inverse cdf F_η^{-1} . In our case we find that a 20th order polynomial chaos expansion suffices to achieve a low error. Fig. 2 shows the resulting expansions evaluated at 1000 sample points ξ or their corresponding $\zeta = 2F_\eta(\mathbf{w}^T \xi) - 1$ accordingly and the density function of the output. Note that in order to obtain a common input domain the plots show the dependence of the expansions with respect to the η sample points.

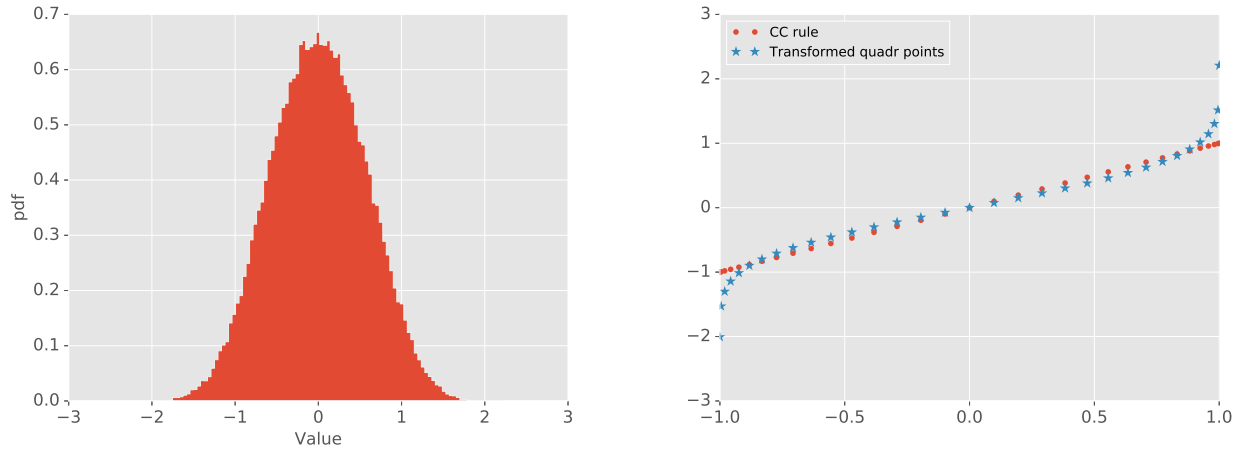


Fig. 1. Left: Plot of the empirical pdf of $\eta = \mathbf{w}^T \xi$ for \mathbf{w} given in eq. (39). Right: Level-5 Clenshaw-Curtis quadrature points on $[-1, 1]$ and their mappings on η -space.

3.2 Multiphase flow: 1d transport and decay of ammonium

Multiphase-multicomponent flow and transport models are known for their particular challenges associated with the uncertainty propagation problem which are mainly due to the highly nonlinear nature of the coupled systems of equations that describe the complex physical process and the varying role of the many random parameters involved in the system. Here we consider the problem of a 1-dimensional transport of the microbially mediated first-order oxidation of ammonium (NH_4^+) to nitrite (NO_2^-) and the subsequent oxidation of nitrite to its ion (NO_3^-) that has been previously investigated in [53, 54, 55]. The flow domain under consideration where the flow of ammonium takes places is taken here to be a one-dimensional column of 2 meters length.

For the numerical solution of the transport and decay model, we employ the multiphase-multicomponent simulator TOUGH2 [56] that solves the integral form of the system of governing equations using the integral finite difference method. More specifically, the EOS7r module [57] that specializes in modeling radionuclide transport, is used here, allowing the

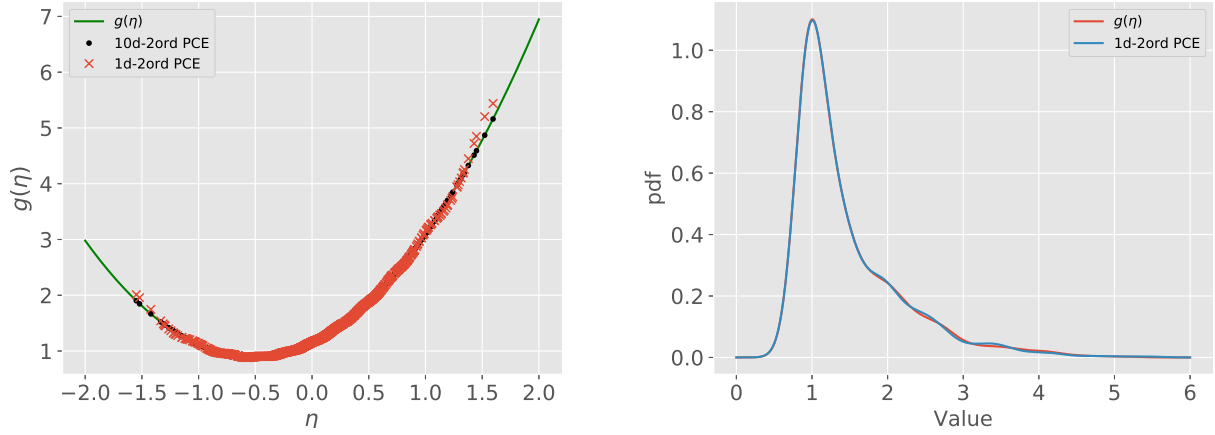


Fig. 2. Left: Predictions of the link function using 1d- and 10d- expansions. Right: Comparison of the true and the estimated density function bases on 1d-20th-order chaos expansion.



Fig. 3. Domain of the ammonium transport problem. Ammonium is injected at $y = 0$.

description of the oxidation effect in a similar manner as specifying half-life parameters to describe radioactive or biodegradation effects. Detailed description of the balance equations and capillary pressure model can be found in [56]. The mass components considered here are water, air, ammonium and nitrite and the fluid phases are aqueous and gas. We consider a first-order decay law for the mass components [57].

In the scenario considered here, the domain is discretized into 400 blocks, each of length 0.005m. and a source of ammonium is placed on the one boundary ($y = 0$), while no concentration of nitrite is initially present. The domain is shown in Fig. 3. Uncertainty is introduced in the model through six model parameters, namely the decay parameters of ammonium and nitrite, $T_{1/2}^{am}$ and $T_{1/2}^{ni}$ respectively, the constant flux of ammonium at the boundary or more precisely the constant injected concentration χ_0^{am} , the distribution coefficient Kd_w^{am} of ammonium that affects its adsorption onto the immobile solid grains and the porosity ϕ of the medium. All other model parameters were assigned fixed values which are shown in Table 1. All random input parameters, denoted in a vector form as $\theta = (T_{1/2}^{am}, T_{1/2}^{ni}, \chi_0^{am}, Kd_w^{am}, \phi)^T$ are assumed to follow uniform distributions $\theta_i \sim \mathcal{U}(\theta_i^l, \theta_i^u)$ where the intervals $[\theta_i^l, \theta_i^u]$, $i = 1, \dots, 5$ are given in Table 2. Next, for the construction of a polynomial chaos approximation of model output, the random input parameters are rescaled to $\mathcal{U}(-1, 1)$ random variables via the transformation

$$\xi_i = 2 \frac{\theta_i - \theta_i^l}{\theta_i^u - \theta_i^l} - 1. \quad (41)$$

Table 1. Material and initial parameters used in my simulations.

Parameter	Symbol	Value
Rock grain density	ρ_R	2650kg/m ³
Tortuosity factor	τ_0	1
Absolute permeability	κ	10 ⁻¹² m ²
Diffusivities (all k): gas phase	d_g^k	10 ⁻⁶
aqueous phase	d_l^k	10 ⁻¹⁰
Molecular weight	-	18
Inverse Herny's constant	-	10 ³⁰
Initial pressure	$P(0)$	1.010 · 10 ⁵
Initial gas saturation	S_g	0.75
Temperature (constant)	T	25°

Table 2. Input parameter value range

Parameter	θ_l	θ_u
$T_{1/2}^{am}$	10 ⁵	10 ⁶
$T_{1/2}^n$	10 ⁴	5 · 10 ⁵
χ_0^{am}	0.008	0.015
$K d_w^{am}$	9 · 10 ⁻⁵	1.1 · 10 ⁻⁴
ϕ	0.2	0.6

3.2.1 Results

The transport model runs for a time period corresponding to $t = 200$ hours and the mass fraction of ammonium in the aqueous phase is observed. The quantity of interest considered here is the mass fraction $\chi_t^{am}(y)$ at the middle point of the column ($y = 1$ m distance from the source), where neglect the index w for simplicity. First, to illustrate the motivation for applying a basis reduction procedure on the QoI, we compute the polynomial chaos expansion of the mass fraction of ammonium over the whole domain $y \in [0, 2]$. Figure 4 shows a comparison of 10 Monte Carlo outputs of the model with the polynomials chaos expansions evaluated at the same MC inputs. The four figures correspond to the cases where the coefficients have been estimated using a Clenshaw-Curtis quadrature rule of level 2, 3, 4 and 5 respectively. Qualitatively we observe that for level 3 and higher, the surrogate is a very good approximation of the model. However, at $y = 1$ we can see that the chaos expansions of $\chi_t^{am}(y)$ fall sometimes below zero which is not an acceptable value since $\chi_t(y)^{am} \geq 0$. This immediately makes the chaos expansion inaccurate not only as a surrogate for fast computation of the model output but will also result in false empirical distributions of the QoI. Next, we use the estimated coefficients for estimation of the gradient matrix G and we denote with G^ℓ the gradient matrix estimated using the coefficients from level ℓ quadrature rule. The eigenvalues and the dominating eigenvector \mathbf{w}^ℓ are shown in Fig. 5. For the cases $\ell = 3, 4$ and 5 the eigenvalues and the vector \mathbf{w}^ℓ almost coincide, indicating convergence of the eigenvalues and existence of a 1-dimensional active subspace. In the $\ell = 2$ case, the eigenvalues seem to be inaccurate and perhaps the projection vector does not define an optimal rotation for dimension reduction. In addition, even though a “gap” can be seen between the first and the remaining eigenvalues, their values indicate that they are not negligible. Fig. 6 (left) shows the 56 estimated coefficients of the expansions for the different quadrature rule levels and similar conclusions can be drawn regarding the convergence of the numerical integration and the accuracy of the expansion, as the level-2 results are completely “off” comparing to the remaining cases and even several coefficients of the level-3 case display some discrepancy before being stabilized in level-4 and level-5 rules.

After defining the random *active* variables $\boldsymbol{\eta}^\ell = \mathbf{w}^{\ell T} \boldsymbol{\xi}$ with cdf $F_{\boldsymbol{\eta}^\ell}(\cdot)$ corresponding to the active subspaces revealed by the chaos expansions estimated above, we construct the PC approximations with respect to the germs

$$\zeta^\ell = 2F_{\boldsymbol{\eta}^\ell}(\boldsymbol{\eta}^\ell) - 1, \quad \ell = 2, \dots, 5, \quad (42)$$

of order 15 using the level-5 1-dimensional CC quadrature rule. The estimated coefficients are displayed in Fig. 6 (right),

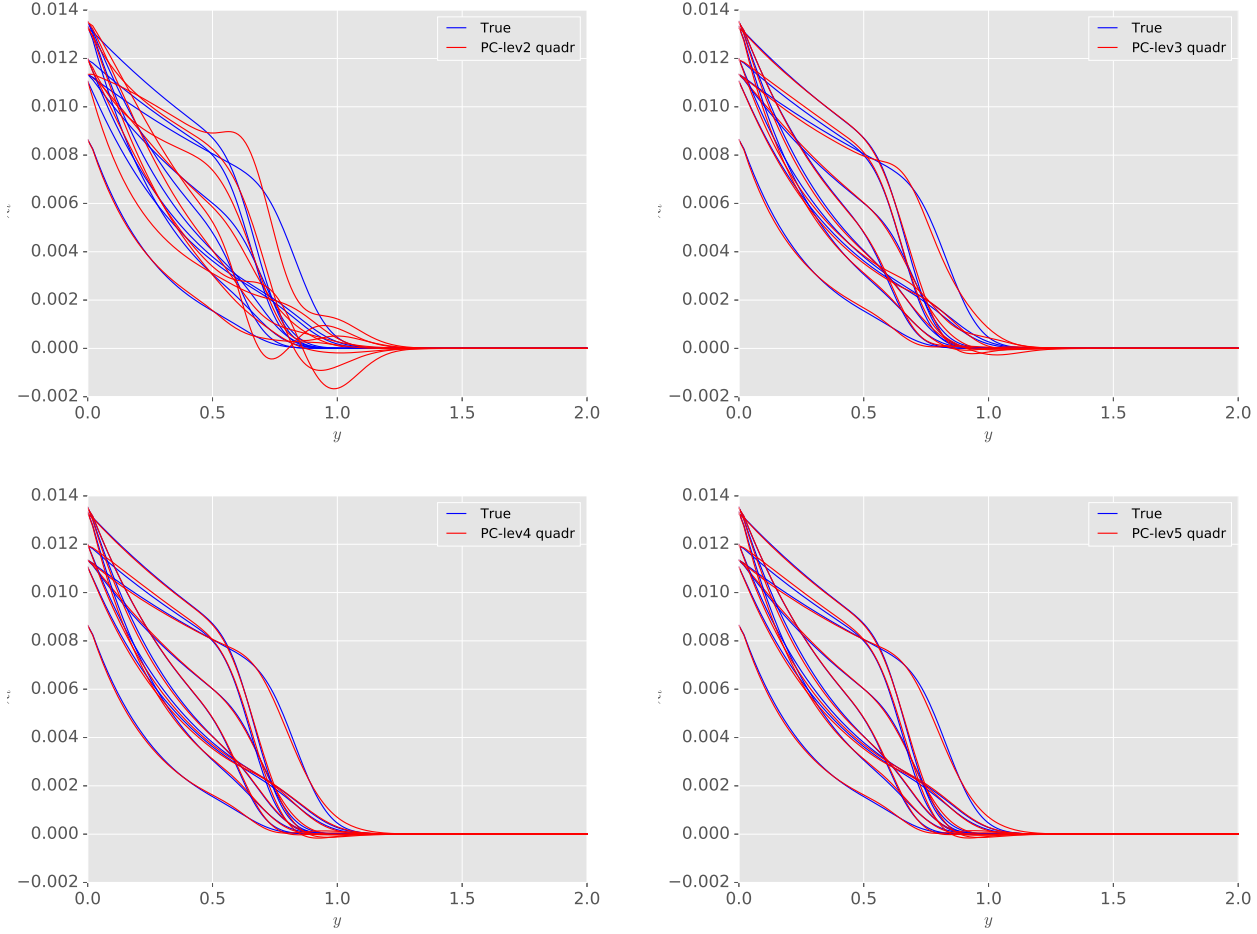


Fig. 4. 10 Monte Carlo realizations of the model outputs and their corresponding PC approximations using quadrature level $\ell = 2, 3, 4$ and 5 respectively.

where except the one corresponding the level 2 rule, they seem to be in good agreement, as expected from the similarity of their respective projection vectors \mathbf{w}^ℓ . Fig. 7 shows values of 1000 MC outputs of the true model and the 1-d PC expansion as a function the common input η^ℓ . Evaluation of the full model is carried out at the points $\xi^{(i)} = \mathbf{w}^\ell \eta^{\ell(i)}$ while evaluation of the 1-d PC expansions is obtained at $\zeta^{(i)} = F_{\eta^\ell}(\eta^{\ell(i)})$. It is observed again that for $\ell \geq 3$, the one dimensional representation of χ_r^{am} provides a quite accurate approximation of the true QoI whose scatter around the 1-d curve due to the influence of the orthogonal subspace $\text{span}\{\mathbf{w}^T \xi\}^T$ is very small.

Finally, we compute the empirical pdfs based on 10^5 MC samples of all 5-d and 1-d PC expansions that we have available and compare their histograms with that of the 1000 MC samples that are available directly from the TOUGH2 model. The results are shown in Fig. 8. It is observed again that those based on the 1-d expansions provide far better approximations of the true histogram which is by definition bounded from below at 0 while those based on the full expansions fail dramatically to capture the lower tail behavior. The computational resources required for the estimation of the expansions described are also in favor of the basis reduction methodology: The 1-d expansion based on an orthogonal projection \mathbf{w} that was computed using $\ell = 3$ quadrature rule required a total of 241 model evaluations for the estimation of the 3rd order 5-d PC plus 33 model evaluations for a level-5 1-d quadrature rule resulting in a total of 274 model evaluations and eventually provides a more accurate density function than a $\ell = 4$, or 5 rule for the full PC that require 801 and 2433 model evaluations respectively!

4 Conclusions

I have presented a methodology that combines the active subspace approach for dimensionality reduction with the construction of polynomial chaos surrogates for the purpose of efficient exploration of response surfaces and uncertainty propagation problems. This approach, serving at the same time as an extension of the basis adaptation framework [45] for Homogeneous Chaos expansions, due to its applicability to generalized Polynomial Chaos, provides an explicit expression of the gradient covariance matrix in terms of the chaos coefficients that allows fast computation of the active subspace that

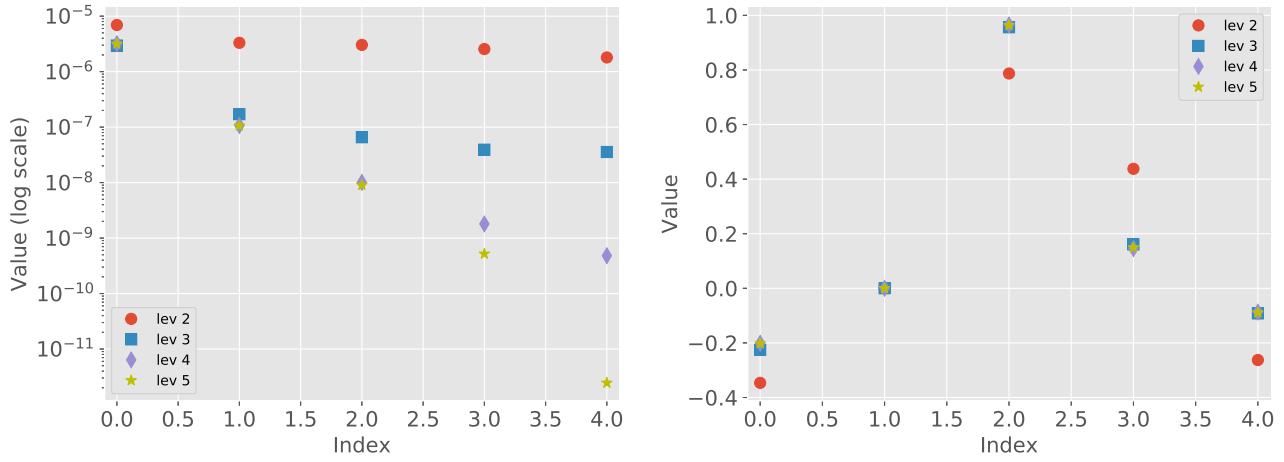


Fig. 5. Eigenvalues of the gradient matrix (left) and the values of the dominant eigenvector \mathbf{w} (right) for chaos coefficients corresponding to different quadrature levels.

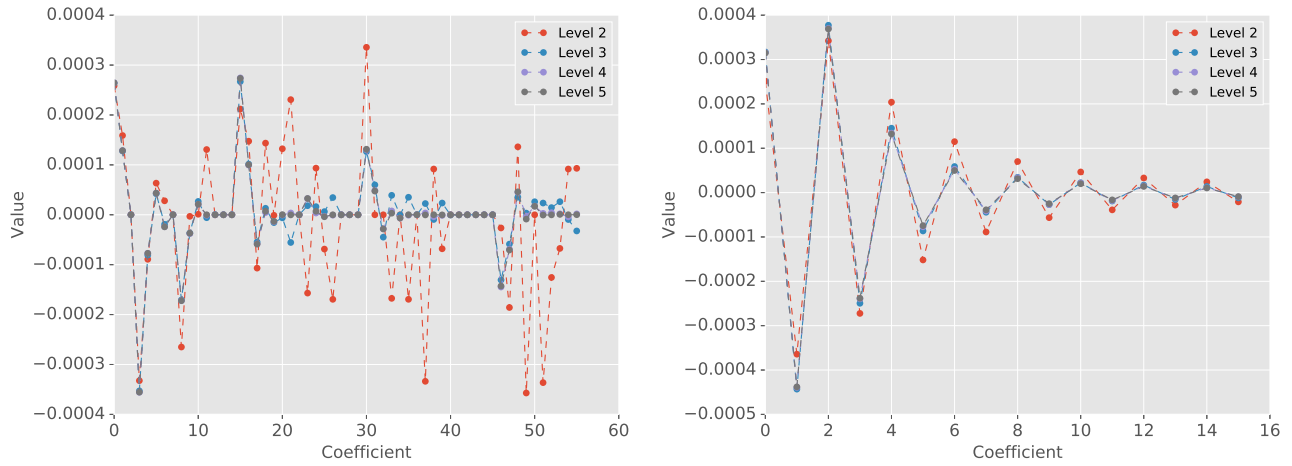


Fig. 6. Estimated coefficients of the chaos expansions using different quadrature rule levels.

is not only useful for dimension reduction, but even for sensitivity analysis purposes. Besides the attractive features in terms of computational efficiency and improved accuracy of the surrogate that were mentioned throughout the manuscript and demonstrated in the numerical examples, the method shows the direction to future challenges: Precisely, the extension of the current approach to higher-dimensional active subspaces, either by finding a way to map the projected variables to a vector of independent ones or by constructing orthogonal polynomials with respect to arbitrary joint distributions, faces several obstacles as detailed in [58] but it would provide a new ground on polynomial chaos-based dimensionality reduction methods.

A Computation of the stiffness matrix K_{ij}

First write the partial derivatives

$$\frac{\partial \psi_{\alpha}(\xi)}{\partial \xi_i} = \frac{\partial}{\partial \xi_i} \prod_{m=1}^d \psi_{\alpha_m}(\xi_m) = \psi'_{\alpha_i}(\xi_i) \prod_{\substack{m=1 \\ m \neq i}}^d \psi_{\alpha_m}(\xi_m). \quad (43)$$

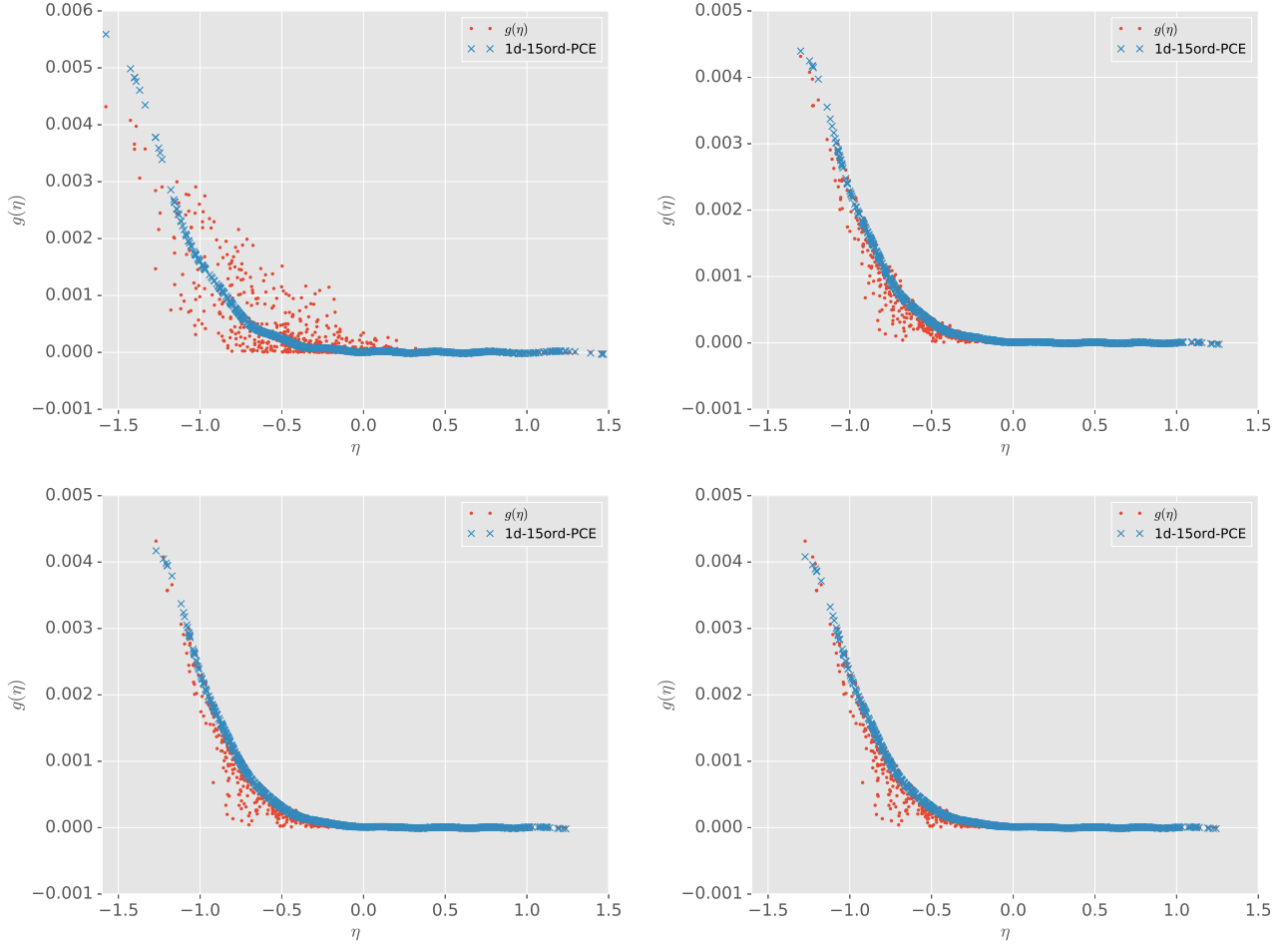


Fig. 7. Evaluation of the model output and the 1-d PC expansions on 1000 MC samples of η^ℓ for $\ell = 2, 3, 4$ and 5 .

Then for any $\alpha, \beta \in \mathcal{I}_P$, we have

$$\begin{aligned}
 (K_{ij})_{\alpha\beta} &= \mathbb{E} \left\{ \frac{\partial \psi_\alpha(\xi)}{\partial \xi_i} \cdot \frac{\partial \psi_\beta(\xi)}{\partial \xi_j} \right\} \\
 &= \mathbb{E} \left\{ \left(\psi'_{\alpha_i}(\xi_i) \prod_{\substack{m=1 \\ m \neq i}}^d \psi_{\alpha_m}(\xi_m) \right) \cdot \left(\psi'_{\beta_j}(\xi_j) \prod_{\substack{m=1 \\ m \neq j}}^d \psi_{\beta_m}(\xi_m) \right) \right\}
 \end{aligned} \tag{44}$$

which for $i \neq j$ gives

$$\begin{aligned}
 (K_{ij})_{\alpha\beta} &= \left(\prod_{\substack{m=1 \\ m \neq i, m \neq j}}^d \mathbb{E} \{ \psi_{\alpha_m}(\xi_m) \psi_{\beta_m}(\xi_m) \} \right) \cdot \mathbb{E} \{ \psi'_{\alpha_i}(\xi_i) \psi_{\beta_i}(\xi_i) \} \cdot \mathbb{E} \{ \psi_{\alpha_j}(\xi_j) \psi'_{\beta_j}(\xi_j) \} \\
 &= \left(\prod_{\substack{m=1 \\ m \neq i, m \neq j}}^d \delta_{\alpha_m, \beta_m} \right) \cdot \mathbb{E} \{ \psi'_{\alpha_i}(\xi_i) \psi_{\beta_i}(\xi_i) \} \cdot \mathbb{E} \{ \psi_{\alpha_j}(\xi_j) \psi'_{\beta_j}(\xi_j) \}
 \end{aligned} \tag{45}$$

and for $i = j$ gives

$$\begin{aligned} (K_{ii})_{\alpha\beta} &= \left(\prod_{\substack{m=1 \\ m \neq i}}^d \mathbb{E} \{ \psi_{\alpha_m}(\xi_m) \psi_{\beta_m}(\xi_m) \} \right) \cdot \mathbb{E} \{ \psi'_{\alpha_i}(\xi_i) \psi'_{\beta_i}(\xi_i) \} \\ &= \left(\prod_{\substack{m=1 \\ m \neq i}}^d \delta_{\alpha_m, \beta_m} \right) \cdot \mathbb{E} \{ \psi'_{\alpha_i}(\xi_i) \psi'_{\beta_i}(\xi_i) \}. \end{aligned} \quad (46)$$

The computation of the terms $\mathbb{E} \{ \psi'_{\alpha}(\xi) \psi_{\beta}(\xi) \}$, and $\mathbb{E} \{ \psi'_{\alpha}(\xi) \psi'_{\beta}(\xi) \}$ depends on the choice of polynomials. The case of Hermite polynomials was derived in [48]. Here I explore the case of Legendre polynomials.

In the case where $\psi_{\alpha}(\xi) = \frac{\ell_{\alpha}(\xi)}{\|\ell_{\alpha}(\xi)\|}$ are the normalized Legendre polynomials, the expectations in the last two terms of the above relation can be computed recursively using the relation

$$(2\alpha + 1)\ell_{\alpha}(\xi) = \frac{d}{d\xi} [\ell_{\alpha+1}(\xi) - \ell_{\alpha-1}(\xi)] \quad (47)$$

that gives

$$\begin{aligned} \mathbb{E} \{ \ell'_{\alpha}(\xi) \ell_{\beta}(\xi) \} &= \delta_{\alpha-1, \beta} + \mathbb{E} \{ \ell'_{\alpha-2}(\xi) \ell_{\beta}(\xi) \} \\ &= \delta_{\alpha-1, \beta} + \delta_{\alpha-3, \beta} + \delta_{\alpha-5, \beta} + \dots \end{aligned} \quad (48)$$

and

$$\begin{aligned} \mathbb{E} \{ \ell'_{\alpha}(\xi) \ell'_{\beta}(\xi) \} &= (2\alpha - 1)\delta_{\alpha-1, \beta-1} + (2\alpha - 1)\mathbb{E} \{ \ell_{\alpha-1}(\xi) \ell'_{\beta-2}(\xi) \} \\ &\quad + (2\beta - 1)\mathbb{E} \{ \ell'_{\alpha-2}(\xi) \ell_{\beta-1}(\xi) \} + \mathbb{E} \{ \ell'_{\alpha-2}(\xi) \ell'_{\beta-2}(\xi) \} \\ &= (2\alpha - 1)(\delta_{\alpha-1, \beta-1} + \delta_{\alpha-1, \beta-3} + \dots) \\ &\quad + (2\alpha - 5)(\delta_{\alpha-3, \beta-1} + \delta_{\alpha-3, \beta-3} + \dots) \\ &\quad + (2\alpha - 9)(\delta_{\alpha-5, \beta-1} + \delta_{\alpha-5, \beta-3} + \dots) + \dots \end{aligned} \quad (49)$$

Using eqs. (48) and (49) finally I compute

$$\mathbb{E} \{ \psi'_{\alpha}(\xi) \psi_{\beta}(\xi) \} = \sqrt{(2\alpha + 1)(2\beta + 1)} \mathbb{E} \{ \ell'_{\alpha}(\xi) \ell_{\beta}(\xi) \} \quad (50)$$

and

$$\mathbb{E} \{ \psi'_{\alpha}(\xi) \psi'_{\beta}(\xi) \} = \sqrt{(2\alpha + 1)(2\beta + 1)} \mathbb{E} \{ \ell'_{\alpha}(\xi) \ell'_{\beta}(\xi) \}. \quad (51)$$

References

- [1] Robert, C., and Casella, G., 2013. *Monte Carlo statistical methods*. Springer Science & Business Media.
- [2] Morokoff, W., and Caflisch, R., 1995. “Quasi-monte carlo integration”. *Journal of computational physics*, **122**, pp. 218–230.
- [3] Tarantola, A., 2005. *Inverse problem theory and methods for model parameter estimation*. SIAM.
- [4] Mosegaard, K., and Tarantola, A., 1995. “Monte carlo sampling of solutions to inverse problems”. *Journal of Geophysical Research: Solid Earth*, **100**, pp. 12431–12447.
- [5] Spall, J. C., 2005. *Introduction to stochastic search and optimization: estimation, simulation, and control*, Vol. 65. John Wiley & Sons.
- [6] Spall, J., 1992. “Multivariate stochastic approximation using a simultaneous perturbation gradient approximation”. *IEEE Transactions on Automatic Control*, **37**.

- [7] Huan, X., and Marzouk, Y., 2013. "Simulation-based optimal bayesian experimental design for nonlinear systems". *Journal of Computational Physics*, **232**, pp. 288–317.
- [8] Tsilifis, P., Ghanem, R., and Hajali, P., 2017. "Efficient bayesian experimentation using an expected information gain lower bound". *SIAM/ASA Journal on Uncertainty Quantification*, **5**, pp. 30–62.
- [9] Ghanem, R., and Spanos, P., 2012. *Stochastic finite elements: A spectral approach, revised edition*. Dover Publications Inc.
- [10] Xiu, D., and Karniadakis, G., 2002. "The wiener-asky polynomial chaos for stochastic differential equations". *SIAM journal on scientific computing*, **24**, pp. 619–644.
- [11] Babuška, I., Nobile, F., and Tempone, R., 2007. "A stochastic collocation method for elliptic partial differential equations with random input data". *SIAM Journal on Numerical Analysis*, **45**, pp. 1005–1034.
- [12] Reagan, M., Najm, H., Ghanem, R., and Knio, O., 2003. "Uncertainty quantification in reacting-flow simulations through non-intrusive spectral projection". *Combustion and Flame*, **132**, pp. 545–555.
- [13] Bilonis, I., and Zabarar, N., 2012. "Multi-output local gaussian process regression: Applications to uncertainty quantification". *Journal of Computational Physics*, **231**, pp. 5718–5746.
- [14] Bilonis, I., Zabarar, N., Konomi, B., and Lin, G., 2013. "Multi-output separable gaussian process: towards an efficient, fully bayesian paradigm for uncertainty quantification". *Journal of Computational Physics*, **241**, pp. 212–239.
- [15] Ma, X., and Zabarar, N., 2009. "An adaptive hierarchical sparse grid collocation algorithm for the solution of stochastic differential equations". *Journal of Computational Physics*, **228**, pp. 3084–3113.
- [16] Saltelli, A., Ratto, M., Andres, T., Campolongo, F., Cariboni, J., Gatelli, D., Saisana, M., and Tarantola, S., 2008. *Global sensitivity analysis: the primer*. John Wiley & Sons.
- [17] Sobol', I., 1990. "On sensitivity estimation for nonlinear mathematical models". *Matematicheskoe Modelirovanie*, **2**, pp. 112–118.
- [18] Owen, A., 2013. "Variance components and generalized sobol' indices". *SIAM/ASA Journal on Uncertainty Quantification*, **1**, pp. 19–41.
- [19] Karhunen, K., 1946. "Über lineare methoden in der wahrscheinlichkeits-rechnung". *Annals of Academic Science Fennicae Series A1, Mathematical Physics*, **37**, pp. 3–79.
- [20] Loève, M., 1955. *Probability Theory*, D. Van Nostrand, Princeton, New Jersey.
- [21] Pearson, K., 1901. "Liii. on lines and planes of closest fit to systems of points in space". *The London, Edinburgh, and Dublin Philosophical Magazine and Journal of Science*, **2**, pp. 559–572.
- [22] Ma, X., and Zabarar, N., 2011. "Kernel principal component analysis for stochastic input model generation". *Journal of Computational Physics*, **230**, pp. 7311–7331.
- [23] Constantine, P., Dow, E., and Wang, Q., 2014. "Active subspace methods in theory and practice: applications to kriging surfaces". *SIAM Journal on Scientific Computing*, **36**, pp. A1500–A1524.
- [24] Constantine, P., Emory, M., Larsson, J., and Iaccarino, G., 2015. "Exploiting active subspaces to quantify uncertainty in the numerical simulation of the hyshot ii scramjet". *Journal of Computational Physics*, **302**, pp. 1–20.
- [25] Lukaczyk, T., Palacios, F., Alonso, J., and Constantine, P., 2014. "Active subspaces for shape optimization". In *Proceedings of the 10th AIAA Multidisciplinary Design Optimization Conference* (pp. 1–18).
- [26] Ghanem, R., 1998. "Scales of fluctuation and the propagation of uncertainty in random porous media". *Water Resources Research*, **34**, pp. 2123–2136.
- [27] Ghanem, R., and Dham, S., 1998. "Stochastic finite element analysis for multiphase flow in heterogeneous porous media". *Transport in Porous Media*, **32**, pp. 239–262.
- [28] Najm, H., 2009. "Uncertainty quantification and polynomial chaos techniques in computational fluid dynamics". *Annual Review of Fluid Mechanics*, **41**, pp. 35–52.
- [29] Le Maître, O., Reagan, M., Najm, H., Ghanem, R., and Knio, O., 2002. "A stochastic projection method for fluid flow: Ii. random process". *Journal of Computational Physics*, **181**, pp. 9–44.
- [30] Xiu, D., and Karniadakis, G., 2003. "Modeling uncertainty in flow simulations via generalized polynomial chaos". *Journal of Computational Physics*, **187**, pp. 137–167.
- [31] Arnst, M., Ghanem, R., and Soize, C., 2010. "Identification of bayesian posteriors for coefficients of chaos expansions". *Journal of Computational Physics*, **229**, pp. 3134–3154.
- [32] Ghanem, R., Doostan, A., and Red-Horse, J., 2008. "A probabilistic construction of model validation". *Computer Methods in Applied Mechanics and Engineering*, **197**, pp. 2585–2595.
- [33] Ghanem, R., and Red-Horse, J., 1999. "Propagation of probabilistic uncertainty in complex physical systems using a stochastic finite element approach". *Physica D: Nonlinear Phenomena*, **133**, pp. 137–144.
- [34] Marzouk, Y. M., Najm, H. N., and Rahn, L., 2007. "Stochastic spectral methods for efficient bayesian solution of inverse problems". *Journal of Computational Physics*, **224**, pp. 560–586.
- [35] Marzouk, Y., and Najm, H., 2009. "Dimensionality reduction and polynomial chaos acceleration of bayesian inference in inverse problems". *Journal of Computational Physics*, **228**, pp. 1862–1902.
- [36] Ghanem, R., and Doostan, R., 2006. "Characterization of stochastic system parameters from experimental data: A

- bayesian inference approach”. *Journal of Computational Physics*, **217**, pp. 63–81.
- [37] Sudret, B., 2007. “Global sensitivity analysis using polynomial chaos expansions”. *Reliability Engineering & System Safety*, **93**, pp. 964–979.
- [38] Crestaux, T., Le Maître, O., and Martinez, J., 2009. “Polynomial chaos expansion for sensitivity analysis”. *Reliability Engineering & System Safety*, **94**, pp. 1161–1172.
- [39] Le Maître, O., and Knio, O., 2015. “Pc analysis of stochastic differential equations driven by wiener noise”. *Reliability Engineering & System Safety*, **135**, pp. 107–124.
- [40] Lucor, D., Meyers, J., and Sagaut, P., 2007. “Sensitivity analysis of large-eddy simulations to subgrid-scale-model parametric uncertainty using polynomial chaos”. *Journal of Fluid Mechanics*, **585**, pp. 255–279.
- [41] Blatman, G., and Sudret, B., 2008. “Sparse polynomial chaos expansions and adaptive stochastic finite elements using a regression approach”. *Comptes Rendus Mécanique*, **336**, pp. 518–523.
- [42] Peng, J., Hampton, J., and Doostan, A., 2014. “A weighted ℓ_1 -minimization approach for sparse polynomial chaos expansions”. *Journal of Computational Physics*, **267**, pp. 92–111.
- [43] Yang, X., and Karniadakis, G., 2013. “Reweighted ℓ_1 minimization method for stochastic elliptic differential equations”. *Journal of Computational Physics*, **248**, pp. 87–108.
- [44] Hampton, J., and Doostan, A., 2015. “Compressive sampling of polynomial chaos expansions: convergence analysis and sampling strategies”. *Journal of Computational Physics*, **280**, pp. 363–386.
- [45] Tipireddy, R., and Ghanem, R., 2014. “Basis adaptation in homogeneous chaos spaces”. *Journal of Computational Physics*, **259**, pp. 304–317.
- [46] Tsilifis, P., and Ghanem, R., 2017. “Reduced wiener chaos representation of random fields via basis adaptation and projection”. *Journal of Computational Physics*, **341**, pp. 102–120.
- [47] Thimmisetty, C., Tsilifis, P., and Ghanem, R., 2017. “Homogeneous chaos basis adaptation for design optimization under uncertainty: Application to the oil well placement problem”. *AI EDAM*, **31**, pp. 265–276.
- [48] Yang, X., Lei, H., Baker, N., and Lin, G., 2016. “Enhancing sparsity of hermite polynomial expansions by iterative rotations”. *Journal of Computational Physics*, **307**, pp. 94–109.
- [49] Tsilifis, P., Huan, X., Safta, C., Sargsyan, K., Lacaze, G., Oefelein, J., Najm, H., and Ghanem, R., 2018. “Compressive sensing adaptation for polynomial chaos expansions”. *arXiv preprint arXiv:1801.01961*.
- [50] Tripathy, R., Bilonis, I., and Gonzalez, M., 2016. “Gaussian processes with built-in dimensionality reduction: Applications to high-dimensional uncertainty propagation”. *Journal of Computational Physics*, **321**, pp. 191–223.
- [51] Tsilifis, P., since 2017. `chaos_basispy`: A Polynomial Chaos basis reduction framework in Python. https://github.com/tsilifis/chaos_basispy.
- [52] Golub, G., and Van Loan, C., 2012. *Matrix computations (Vol. 3)*. JHU Press.
- [53] Cho, C., 1971. “Convective transport of ammonium with nitrification in soil”. *Canadian Journal of Soil Science*, **51**, pp. 339–350.
- [54] McNab, W., and Narasimhan, T., 1993. “A multiple species transport model with sequential decay chain interactions in heterogeneous subsurface environments”. *Water Resources Research*, **29**, pp. 2737–2746.
- [55] Van Genuchten, M., 1985. “Convective-dispersive transport of solutes involved in sequential first-order decay reactions”. *Computers & Geosciences*, **11**, pp. 129–147.
- [56] Pruess, K., Oldenburg, C., and Moridis, G., 1999. *TOUGH2 User’s guide, Version 2*. Berkeley, California. Report LBNL-43134.
- [57] Oldenburg, C., and Pruess, K., 1995. *EOS7R: Radionuclide transport for TOUGH2*. Berkeley, California, November. Report LBL-34868.
- [58] Soize, C., and Desceliers, C., 2010. “Computational aspects for constructing realizations of polynomial chaos in high dimension”. *SIAM Journal on Scientific Computing*, **32**, pp. 2820–2831.

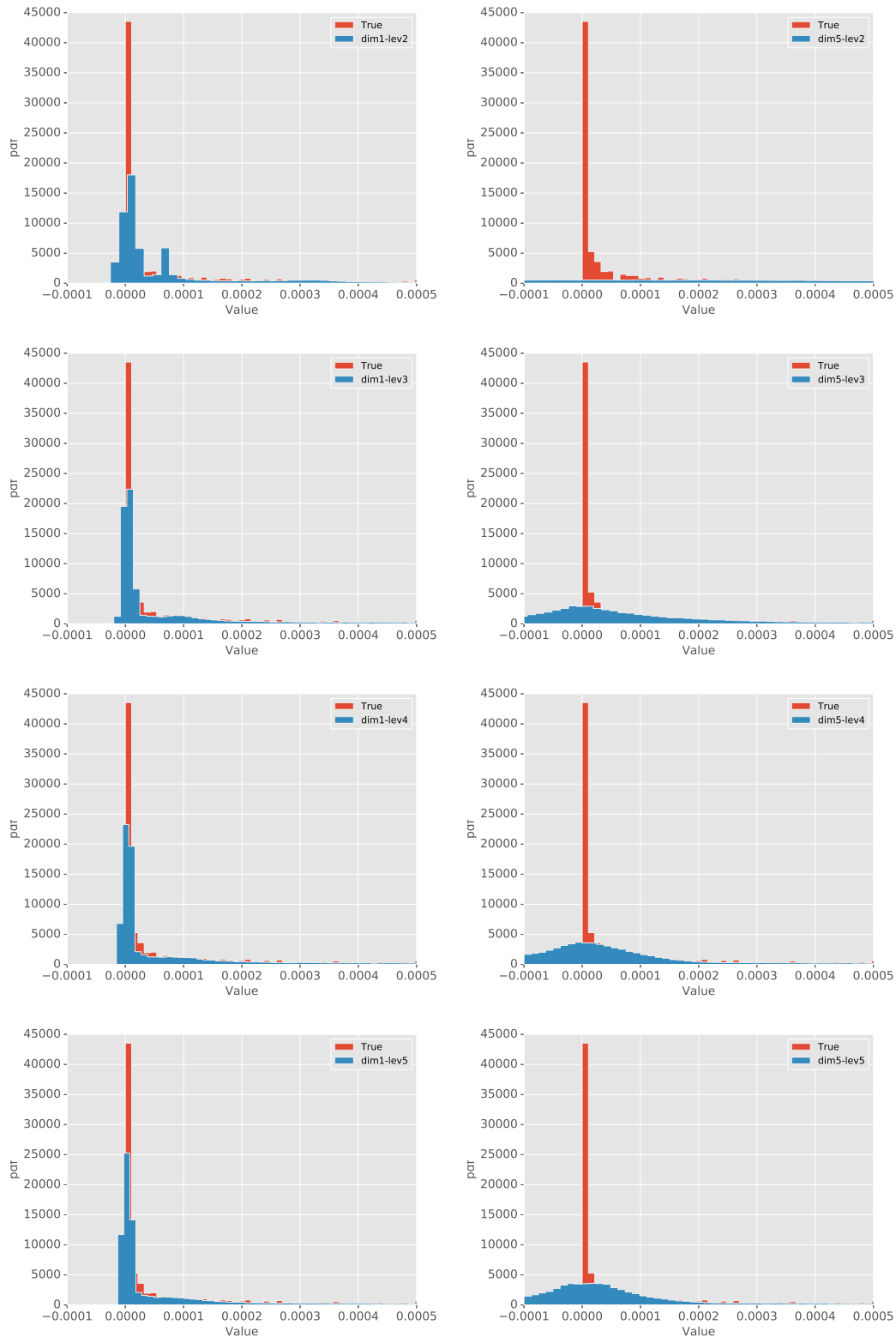


Fig. 8. Histogram comparison based on MC samples from the 1d- (left column) and 5d- (right column) chaos expansions with that based on 1000 MC samples drawn from the TOUGH2 simulator (all histograms are normalized such that the bins integrate to 1).